

# Heat Transfer Enhancement Through Different Heat Sink/Impinging Air Jet Parameters an Experimental Approach

M'hamed BERIACHE\*, Brahim Hicham CHERKI\*, Leila MOKHTAR SAÏDIA\*, Che Sidik NOR AZWADI\*\*, Mamat RIZALMAN\*\*\*

\*Laboratory of Rheology and Mechanics, Department of Mechanical Engineering, Faculty of Technology, Hassiba Benbouali University of Chlef, Algeria, E-mail: m.beriache@univ-chlef.dz (Corresponding author)

\*\*Malaysia–Japan International Institute of Technology (MJIT), University Teknologi Malaysia Kuala Lumpur, Jalan Sultan Yahya Petra, 54100 Kuala Lumpur, Malaysia, E-mail: azwadi@mail.fkm.utm.my

\*\*\*Faculty of Mechanical Engineering, University Malaysia Pahang, 26600 Pekan, Pahang, Malaysia, E-mail: rizalman@ump.edu.my

**crossref** <http://dx.doi.org/10.5755/j02.mech.31929>

## Nomenclature

$A$  – section of the heat sink channel, mm<sup>2</sup>;  $A_t$  – heat exchange surface, mm<sup>2</sup>;  $A_f$  – surface of the fin, mm<sup>2</sup>;  $D_h$  – hydraulic diameter, mm;  $H_s$  – heat sink height, mm;  $H$  – air jet height, mm;  $h$  – convection heat transfer coeff., W/m<sup>2</sup>.K;  $h_a$  – fin height, mm;  $h_b$  – thickness of heat sink base, mm;  $L$  – length of fin, mm;  $l_a$  – thickness of the fin, mm;  $l_c$  – channel width, mm;  $P_m$  – wet perimeter, mm;  $N$  – number of fin;  $Q_{elec}$  – heat source power, W;  $Q_{conv}$  – convection thermal power, W;  $Q_{rad}$  – radiation thermal power, W;  $Q_{loss}$  – thermal power loss, W;  $T_j$  – junction temperature, °C;  $T_{amb}$  – ambient temperature, °C;  $T_{jet}$  – temperature of the impinging air jet, °C;  $V$  – air jet velocity, m/s;  $W$  – heat sink width, mm;  $\nu$  – kinematic viscosity, m<sup>2</sup>/s;  $\rho$  – density of fin material, kg/m<sup>3</sup>.

## 1. Introduction

It is noted that the manufacture of electronic components in recent years' records that it has become more and more advanced in terms of functionality, but it is getting smaller in terms of size. Which makes it more compact. This situation resulted in a steady increase in the generated heat [1-4]. As a result, getting rid of excess heat and enabling electronic chips to operate under safe temperatures has become a vital solution in operating electronic components in a reliable and safe manner [5, 6]. The standard cooling techniques used today are sometimes insufficient because of the lack of optimization of the various parameters involved in the cooling process. On the other hand, the inherent advantages of miniature channel heat sinks have allowed these systems to become more and more important in small-scale cooling techniques. Micro-technologies are gaining momentum in our daily lives [7, 8]. In most cases, conventional cooling in the field of electronics depends on solutions that combine impingement air jet with a heat sink, this technology has proven its advantages in terms of reliable performance and low cost. However, the most frequent cooling technique in this field is that using the pairing between an air jet and a mini or micro channel heat sink. The design of a good cooling solution must consider certain factors such as simplicity, price and performance, mainly the thermal resistance provided by the system [9-11]. Adil et al. [12] have been carried out an experimental and numerical investigation on CPU cooling with air jet impinging minichannel heat

sink. The heat transfer coefficient was improved to minimize energy consumption. In a numerical study, Alam et al. [13] evaluated the thermofluid characteristics of a triangular-shaped pin-fin micro heat sink for CPU air-cooling. The effect of fin diameter at different Reynolds numbers has been studied. According to the results, it is proved that the Nusselt number (Nu) increases with the increase of the cooling air velocity, which consequently improves the heat extraction from the CPU. In an experimental study carried out by Hao et al. confirm the positive contributions of minichannel heat sinks subject to air impacting jet as a CPU cooling system [14]. Wang et al. In this work, the authors have numerically analyzed the aero-thermal behavior of three pin fin heat sink with centered vertical jet inlets and multiple outlets. The results are compared with those of the traditional (control) cross-flow heat sink. It is shown that the heat sink subjected to a vertical jet with four outputs has the best performance [15]. Beriache et al. [16] numerically predicted the thermal performance of a rectangular mini-channel heat sink cooled by an impingement air jet in a laminar regime. The junction temperature as well as the thermal resistance and pressure drop of the heat sink were investigated as a function of the Reynolds number. Yang et al. [17] computationally studied the turbulent fluid flow and heat transfer characteristics of air jet impingement on the rotating and stationary squared pin-fin heat sink. Huang and Chen [18, 19] used the Levenberg-Marquardt method to size the heat sink in order to optimize its geometric characteristics. Yu et al. [20] experimentally and computationally investigated the heat transfer and fluid flow behaviour of air jet impingement in heat sinks by proposing the integration of piezoelectrically-driven agitators and synthetic jets within air-cooled heat sinks. Barrau et al. [21] conducted an experimental study, in which they examined the effect of the geometric shape of the nozzle on the characteristics of a combined jet-impingement/microchannel cooling system. Byon [22] experimentally investigated the jet impingement heat transfer features of aluminum foam heat sinks. The influence of the blowing power, the flow velocity as well as the impact height of the jet on the thermal performance are examined. Lin et al. [23] proposed the optimum design and heat transfer correlation of a mini-radiator with liquid jet impingement for the CPU cooling. Xia et al. [24] have used experience and computer to study the fluid flow and heat transfer characteristics in complex structure microchannel heat sink. In this work, we examine experimentally a cooling system

of power electronic components based on minichannel heatsink subjected to impinging air jet. It is a question of testing and characterizing a commercial cooling system. Then, we examine the potential for improving its dynamic and thermal performance. A parametric study for the cooling characteristic investigation of a personal computer central processor unit (CPU) has been experimentally performed. The effect of height cooling air flow, airflow, blowing and suction patterns, and the influence of air duct shape on thermal and dynamic performance was tested and discussed in order to improve the current commercial cooling system.

## 2. Experimental equipment

The experimental test setup shown in Fig. 1 and used in the accomplishment of this work, consists essentially of an impinging air jet system, a minichannel heat sink and a number of devices intended to measurement of airflow velocity as well as air and heat sink temperature. The air jet with a jet diameter  $D = 66$  mm is generated by a mini axial fan with a size of  $70 \times 70 \times 15$  mm, operating at 12VDC 0.7A, which can provide up to  $42 \text{ m}^3/\text{h}$  of air. Its power supply is ensured by an adjustable DC generator, which allows the velocity of the fan to be varied according to the supply voltage. Airflow is routed from the fan to the heatsink along Plexiglas ducts of different heights as well as different shapes.

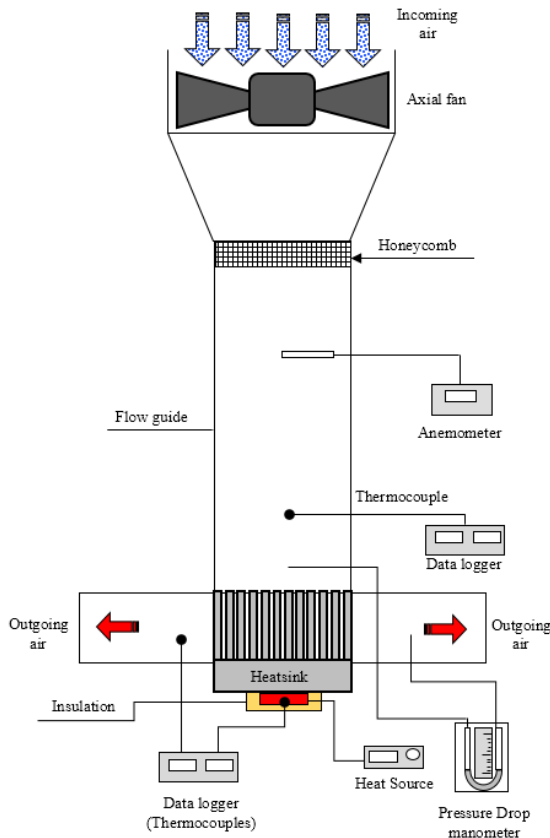


Fig. 1 Experimental test bench

The plate fin minichannel heat sink tested in this experiment is made of pure extruded aluminum (Fig. 2), it is characterized by a low density  $\rho = 2702 \text{ kg/m}^3$ , i.e. a light weight with a high thermal conductivity, around  $237 \text{ W/m.K}$  [25].

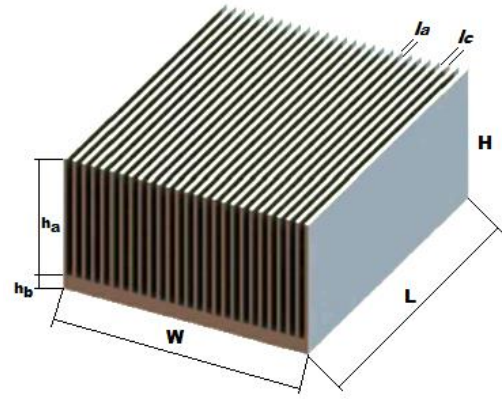


Fig. 2 Rectangular minichannel plate fin heat sink

The dimensions of the heat sink are shown in Table 1 below.

Table 1

Heat sink dimensions, mm

$N$	$W$	$h_a$	$L$	$h_b$	$l_c$	$l_a$	$H$
27	66	32	82	4	1.5	1	36

At the bottom of the heat sink is fixed a heating element (heat source) with dimensions  $35 \times 35 \times 15$  mm, generating a thermal power of 80 Watt simulating the central processing unit (CPU). This heat source is securely attached to the base of the heatsink via a clamp system. Good contact is ensured between these two elements by the application of a thermal paste. The heat sinks and heat source assembly is subjected to the impinging air jet provided by the axial fan. The experimental setup of Fig. 1 allows adjustment of the jet at different blowing heights namely;  $H = 0$  mm,  $H = 20$  mm,  $H = 40$  mm,  $H = 60$  mm and  $H = 80$  mm and even test air duct types with different geometry and see their effects on cooling system efficiency.

## 3. Experimental measurements procedure

The measurement of the air temperature at different stations as well as those of the heat sink is carried out by type  $K$  thermocouples  $\varnothing 0.2$  mm, connected to a Kimo TM200 digital thermometer, with an accuracy of  $\pm 0.4\%$  (Fig 1). As for the measurement of the airflow velocity through the heat sink channels, it is performed using a Kimo VT200 type hot wire anemometer probe moving perpendicular to the axis of the heatsink channel, the instrument having an accuracy of  $\pm 0.3\%$ . The pressure loss across the heat sink,  $\Delta p = p_{in} - p_{out}$ , is sensed using a Kimo MP100 differential pressure gauge with digital display, having two pressure taps, one mounted at the inlet and the other at the output of the heatsink, its accuracy is rated at  $\pm 0.5\%$ . Several mean flow velocities, ranging from  $0.5 \text{ m/s}$  to  $3.5 \text{ m/s}$ , under a laminar flow regime through the dissipating channels, are indeed tested. The experiment is carried out in an air-conditioned enclosure at an ambient temperature of  $23^\circ\text{C}$ .

## 4. Parameters of calculation

The study represents a forced convection problem under steady-state laminar airflow conditions. The nature of flow is characterized by evaluating the Reynolds number, as follows:

$$R_e = \frac{V \cdot D_h}{\nu}, \quad (1)$$

where,

$$D_h = \frac{4A}{P_m} = \frac{2h_a l_c}{h_a + l_c}. \quad (2)$$

With,  $D_h$  is the hydraulic diameter and  $A$  is the cross section of the heat sink channel.

The heat balance of the cooling system and its surrounding external environment in the steady state can be drawn up as follows:

$$Q_{elec} = Q_{conv} + Q_{rad} + Q_{loss}, \quad (3)$$

where:  $Q_{elec}$  is the electrical power supplied to the heat source (CPU), which is fixed at the base of the heat sink. While,  $Q_{conv}$ ,  $Q_{rad}$ , are the thermal power of the cooling system by convection and by radiation respectively. As for  $Q_{loss}$ , it represents the thermal losses.

The radiation thermal power  $Q_{rad}$  resulting from the considered heat sink, is evaluated according to the following relation [2]:

$$Q_{rad} = \sigma F A_s (T_w^4 - T_{amb}^4). \quad (4)$$

With,  $\sigma$  is Stefan-Boltzmann constant and  $F$  is the geometric form factor and  $T_w$  is the wall temperature.

According to the data available on the heat sink made of Aluminum with highly polished surface, this allows to minimize its emissivity. Consequently, the thermal radiative losses  $Q_{rad}$  can be neglected in the calculations below. To reduce thermal losses  $Q_{loss}$ , applying good thermal insulation to the heat source as well as the base of the heat sink minimize these losses. Conferring to [14], thermal losses are assessed as following:

$$Q_{loss} = \frac{A \cdot K_{ins}}{\Delta x} \Delta T_{ins}. \quad (5)$$

With  $A$  is the surface of the base of the heat sink,  $K_{ins}$  is the insulation thermal conductivity,  $\Delta T_{ins}$  represents the temperature gradient across the insulating medium and  $\Delta x$  is the insulation thickness.

The convective heat transfer coefficient  $h$  is calculated according to [14] as follows:

$$h = \frac{Q_{conv}}{A_t [T_j - T_{jet}]} = \frac{Q_{elec} - Q_{loss}}{A_t [T_j - T_{jet}]}. \quad (6)$$

With,  $T_{jet} \approx T_{amb}$  and  $A_t$  is the heat exchange surface, expected conferring to [26, 27] by the relation:

$$A_t = N A_f + A_b. \quad (7)$$

As for the thermal resistance representing the key performance, it is expressed as follows:

$$R_{th} = \frac{T_j - T_{jet}}{Q_{elec} - Q_{loss}}. \quad (8)$$

## 5. Results and discussions

### 5.1. Effect of impingement jet height on the velocity profile

According to Fig. 3, the velocity of the cooling air jet incident in the heat sink considered has the lowest values at the level of the central zone of the heat sink, which unfortunately corresponds to the heat source position. This result is a consequence to the passive area below the axial fan motor, thus causing a low cooling area (see the line of symmetry in Fig. 3). Unfortunately, this area of poor airflow is the hottest area on the heatsink, because the heat source is attached there, another suspect factor and which could be explained by the fact that the spacing between the jet and the radiator becomes confined, thus preventing the jet from expanding sufficiently to provide the radiator with adequate cooling. To remedy this problem, an attempt is examined, by varying the height of the jet and seeing its effect on the velocity profile giving a good blow in this area. It is recorded that, when the fan is operational at a constant speed, the blowing speed profile which best corresponds to the need to obtain better heat dissipation, corresponds to the ratio  $H/D = 0.303$ , i.e. a Jet height  $H = 20$  mm.

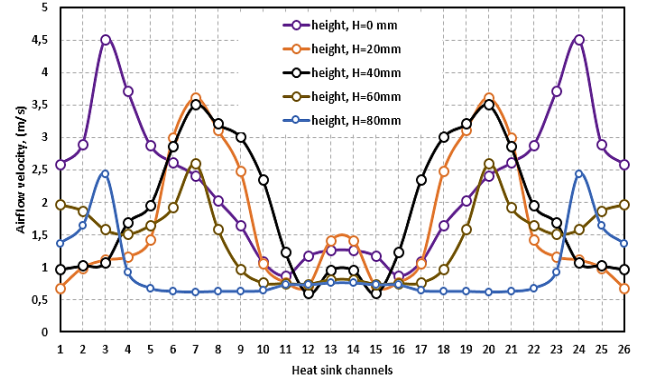


Fig. 3 Velocity of the air jet versus the height of the jet

### 5.2. Effect of air impingement jet height on the junction temperature

Fig. 4 demonstrates the evolution of the junction temperature at the level of the heat source at the bottom of the heat sink during start-up and until the establishment of the steady state. According to the results of Fig. 4, the evolution of the junction temperature increases rapidly during a transient state spanning 360 sec, then stabilizes permanently. The results prove that the height of the jet as well as the type of duct channeling the cooling air have a clear influence on the junction temperature (Fig. 7). A first reading reveals that a jet with a duct of 20 mm height has a better cooling advantage of CPU (central processor unit) of around 10% improvement compared to other jet ducts of different heights. A second reading of the results (Fig. 7) reveals that the use of a convergent duct further improves the cooling rate by an additional approximately 8% and this is due to its air flow concentrator effect towards the hot zone (heat source). This advantage is more significant with regard to the use of a hair dryer duct by ensuring more improvement in cooling of the junction temperature, this improvement is

evaluated at 1.1% more. In conclusion, the improvement in the rate of cooling recorded is about 19% between a jet of air blowing from a height of 80 mm and a jet of air concentrated by a hair dryer duct.

This significant gain is the result of improving the flow of cooling air at the level of the stagnation zone previously located above the heat source by studying the velocity profiles through the heat sink.

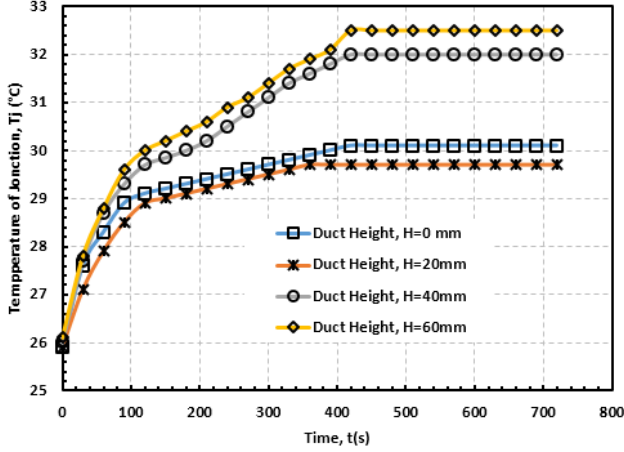


Fig. 4 Junction temperature versus the jet height

### 5.3. Cooling performance test with convergent duct and hair dryer type duct

The problem of heat concentration in the center of the heatsink as well as the poor air circulation in this place, which has been reported since the beginning of this study, led us to look for a solution to improve heat transfer rate in this area by examining a convergent air duct and a hair dryer type duct, see Fig. 5, which act as air concentrators used to guide the flow of air towards the center of the radiator, place of heat accumulation.

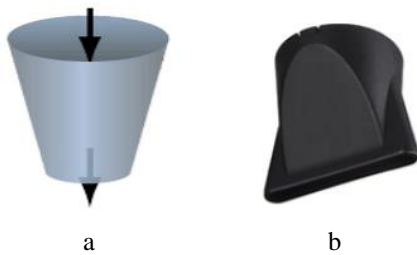


Fig. 5 Convergent duct (a) and hairdryer type duct (b)

Indeed, it can be seen from Fig. 6, that for a constant operating velocity of the fan, the blowing velocity profile that best meets the concern of obtaining a better possible heat transfer, corresponds conduit hair dryer. The velocities from the hair dryer tip far exceed those from the best standard pipe height,  $H = 20$  mm. That said, the improvement of the flow in the central zone is substantially achieved, which will consequently improve the heat dissipation in this zone.

Fig. 7 shows the comparison of the junction temperature results resulting from the use of the convergent duct, the hair dryer nozzle duct and the optimal ordinary duct of height  $H = 20$  mm. On the light of these results, we see that the convergent duct of height  $H = 40$  mm provides a significant improvement in terms of junction temperature that does not exceed  $27.5^{\circ}\text{C}$ , as for the convergent duct height  $H = 60$  mm provides a junction temperature not exceeding  $27.7^{\circ}\text{C}$ . On the other hand, the conduit hair dryer

gives the lowest junction temperature that does not exceed  $27.4^{\circ}\text{C}$ , against a temperature of  $29.7^{\circ}\text{C}$  for the ordinary conduit height  $H = 20$  mm.

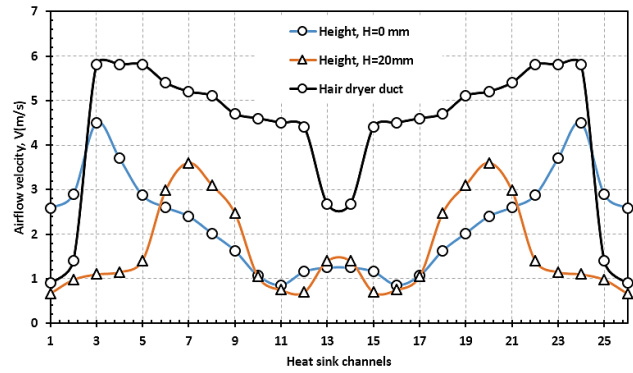


Fig. 6 Jet velocity profiles for ordinary duct,  $H = 20$  mm and for duct nozzle hair dryer

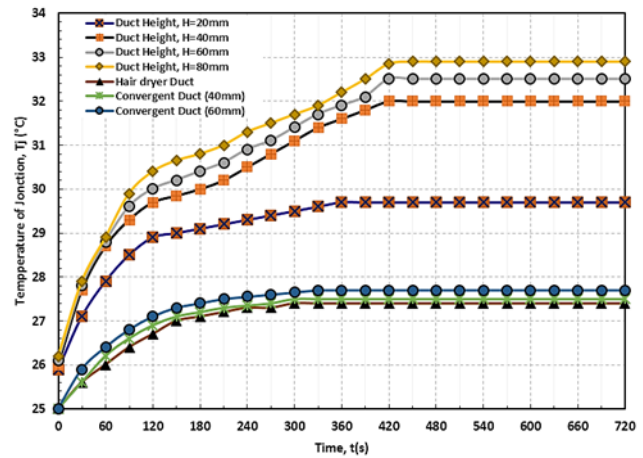


Fig. 7 Junction temperatures from ducts: ordinary, convergent and dry hair duct

It can be seen that the hairdryer records the shortest transient heating time with a maximum junction temperature not exceeding  $27.4^{\circ}\text{C}$ . This is a clear improvement in the performance of the cooling system.

### 5.4. Effect of fan operating mode

In this section, we examine our cooling technique in suction mode since the operation in discharge mode has already been tested previously. The test only concerns the use of two main ducts, that of height  $H = 0$  mm (marketed CPU cooling system) and  $H = 20$  mm (improved CPU cooling system). The results obtained (Fig. 8) show that the operation of the fan in suction mode is more efficient than in blowing mode for different pipe heights on one side and that the pipe height  $H = 20$  mm is better in this mode than height  $H = 0$  mm on the other side.

According to the results, the 20 mm high duct gave us a junction temperature not exceeding  $30^{\circ}\text{C}$  versus a temperature above  $30^{\circ}\text{C}$  for the other duct. Thus, this experimental result is original. It shows the superiority of the proposed cooling system over the marketed one. However, this result may have a potential impact in the forced air convection cooling systems industry.

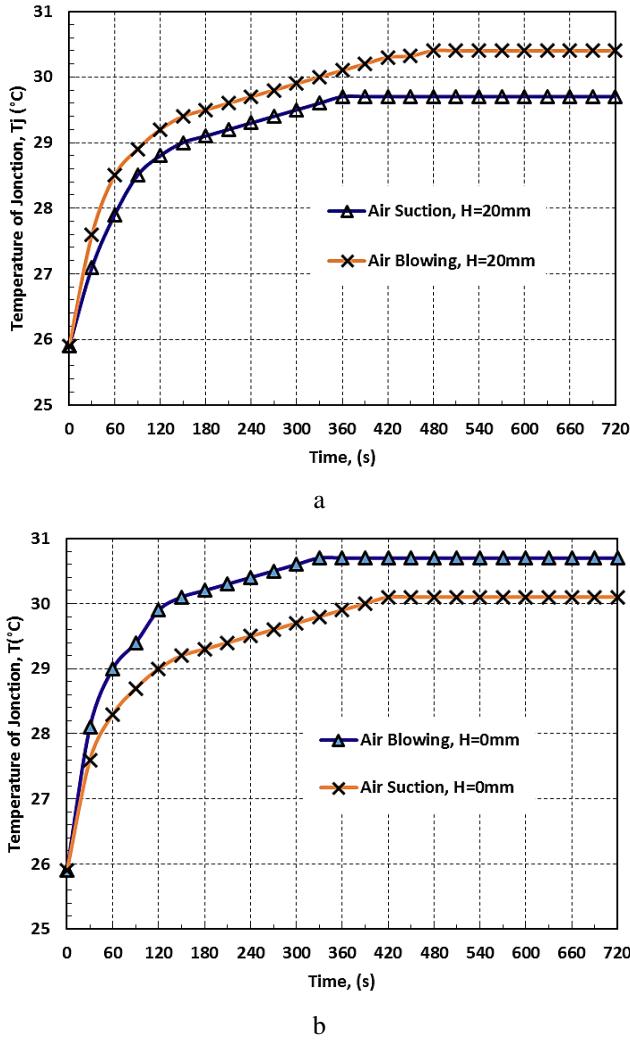


Fig. 8 Junction temperature versus the jet airflow mode (a) for  $H = 20$  mm (b) for  $H = 0$  mm

### 5.5. Thermal resistance as function of air jet velocity

The thermal resistance parameter is a key thermal performance. Fig. 9 shows the progress of the thermal resistance versus of the air jet mean velocity. From the results, in the case of a duct with a height of 20 mm, it is clearly noted that, as the air jet velocity increases, the thermal resistance decreases, initially with a significant slope until the velocity reaches 2.25 m/s, then declines and progresses with a smaller slope than before. This drop in thermal resistance, demonstrates the increase in heat removal capacity.

Whereas, for convergent ducts of variable height as well as for the hair dryer duct, the thermal resistance of the cooling system is significantly lower than that resulting from the former duct with 20 mm of height. In addition, it is not too dependent on the cooling rate, i.e. these last two types of ducts give the cooling system a better performance with a low blowing energy consumption.

### 5.6. Heat transfer coefficient

Moreover, the heat transfer coefficient by convection represents an important element among the studied performances of the cooling system. Indeed, Fig. 10 shows the evolution of the convective heat transfer coefficient versus of airflow jet cooling velocity. Increasing the blowing velocity induces a proportional increase in the convection heat

transfer coefficient. That said, increasing air cooling velocity provides more heat removal. According to Fig. 10, it is noted that the duct which offers the best heat transfer coefficient for our cooling system is the hair dryer duct. With a value approaching 180 watts/m<sup>2</sup>.K. for a blowing velocity of 3.35 m/s. This solution offers a significant improvement ranging from 87.5% to 630.8% compared to the duct ensuring a jet height  $H = 20$  mm which is more improved in characteristics than the commercial configuration ( $H = 0$  mm).

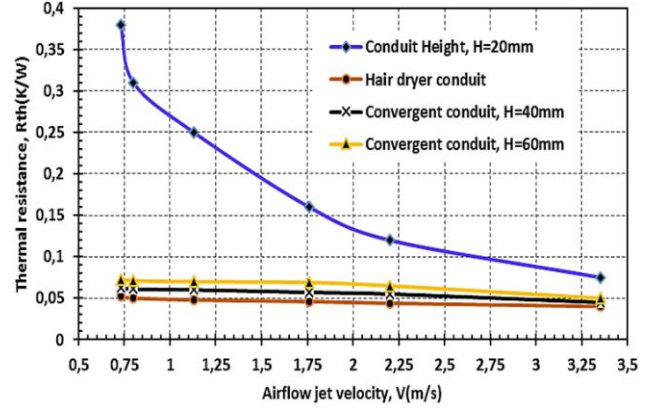


Fig. 9 Thermal resistance versus the air jet velocity

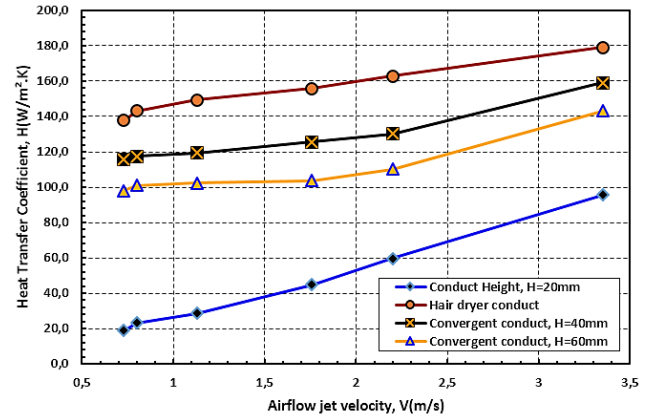


Fig. 10 Heat transfer coefficient versus air jet velocity

## 6. Conclusion

From the work carried out, the following conclusions are made:

- It is found that the blowing height of the adequate air jet giving a better air circulation above the hot zone is  $H = 20$  mm.
- It is concluded that the height duct ( $H = 20$  mm) records the shortest transient heating time with a maximum junction temperature not exceeding 29.7°C. Therefore, we can conclude that the heating element (CPU) is well cooled based on the restrictions recommended by the manufacturer Intel® (P4, 3GHz, 80 W),  $T_{max} < 70^\circ\text{C}$ .
- The operation of the fan in the suction mode is more efficient than in the blowing mode for the different duct heights on one side and the duct height  $H = 20$  mm is better in this mode than that of the traded configuration in height ( $H = 0$  mm) on the other side.
- The use of a convergent duct and a hair dryer type duct shows that the velocities from the hair dryer far exceed those from the best standard pipe height,  $H = 20$  mm. That means, the improvement of the airflow in the central zone is substantially achieved, which consequently

improves the heat removal in this zone which consequently improves the heat transfer in this zone at least 19% compared to the initial trade solution.

### Acknowledgements

The authors would like to thank the General Directorate of Scientific Research and Technological Development (DGRSDT), as well as the faculty of technology at Hassiba Benbouali University of Chlef for providing them with financial support and providing the equipment and facilities needed to accomplish this study. This study is part of research projects (PRFU, 2019-2022) funded by the Algerian Ministry of Higher Education and Scientific Research.

### References

- Hung-Yi, L.; Ci-Lei, C.; Shung-Ming, C.; Gu-Fan, L.** 2013. Enhancing heat transfer in a plate-fin heat sink using delta winglet vortex generators, *International Journal of Heat and Mass Transfer* 67: 666–677. <https://doi.org/10.1016/j.ijheatmasstransfer.2013.08.042>.
- Cheng-Hung, H. A.; Yu-Hsiang, C. A.; Hung-Yi, L.** 2013. An impingement heat sink module design problem in determining optimal non-uniform fin widths, *International Journal of Heat and Mass Transfer* 67: 992-1006. <https://doi.org/10.1016/j.ijheatmasstransfer.2013.08.103>.
- Hussain, A. A.; Freegah, B.; Khalaf, B. S.; Towsyfyhan, H.** 2019. Numerical investigation of heat transfer enhancement in plate-fin heat sinks: Effect of flow direction and fillet profile. *Case Studies in Thermal Engineering* 13: 100388. <https://doi.org/10.1016/j.csite.2018.100388>.
- Li, H. Y.; Chiang, M. H.; Lee, C. I.; Yang, W. J.** 2010. Thermal performance of plate-fin vapor chamber heat sinks. *Int. Commun. Heat Mass Transf.*, 37 (7): 731-738. <https://doi.org/10.1016/j.icheatmasstransfer.2010.05.015>.
- Beriache, M.; Bettahar, A.; Loukarfi, L.; Mokhtar Saïdia, L.; Naji, H.** 2011. Numerical study on hydraulic and thermal characteristics of a minichannel heat sink with impinging air flow, *Mechanika* 17(2): 156-161. <https://doi.org/10.5755/j01.mech.17.2.331>.
- Nilpueng, K.; Mesgarpour, M.; Asirvatham, L. G.; Dalkılıç, A. S.; Ahn, H. S. Mahian, O.; Wongwises, S.** 2021. Effect of pin fin configuration on thermal performance of plate pin fin heat sinks. *Case Studies in Thermal Engineering* 27: 101269. <https://doi.org/10.1016/j.csite.2021.101269>.
- Ahmed, H. E.; Salman, B. H.; Kherbeet, A. Sh.; Ahmed, M. I.** 2018. Optimization of thermal design of heat sinks: A review. *International Journal of Heat and Mass Transfer* 118: 129-153. <https://doi.org/10.1016/j.ijheatmasstransfer.2017.10.099>.
- Nakharintr, L.; Naphon, P.; Wiriyasart, S.** 2018. Effect of jet-plate spacing to jet diameter ratios on nanofluids heat transfer in a mini-channel heat sink, *International Journal of Heat and Mass Transfer* 116: 352-361. <http://dx.doi.org/10.1016/j.ijheatmasstransfer.2017.09.037>.
- Khudhur, D. S.; Al-Zuhairy, R. Ch.; Kassim, M. S.** 2022. Thermal analysis of heat transfer with different fin geometry through straight plate-fin heat sinks, *International Journal of Thermal Sciences* 174: 107443. <https://doi.org/10.1016/j.ijthermalsci.2021.107443>.
- Wiriyasart, S.; Naphon, P.** 2019. Liquid impingement cooling of cold plate heat sink with different fin configurations: High heat flux applications. *International Journal of Heat and Mass Transfer* 140: 281-292. <https://doi.org/10.1016/j.ijheatmasstransfer.2019.06.020>.
- Wang, J.; Kong, H.; Xu, Y.; Wu, J.** 2019. Experimental investigation of heat transfer and flow characteristics in finned copper foam heat sinks subjected to jet impingement cooling. *Applied Energy* 241: 433-443. <https://doi.org/10.1016/j.apenergy.2019.03.040>.
- Adil, M.; Khan, A.; Gupta, A.; Ahmad, S.; Altamush Siddiqui, M.** 2021. Experimental and Numerical Studies of Heat Transfer Through Heat Sinks in Electronic Devices. In: Saran, V.H., Misra, R.K. (eds) *Advances in Systems Engineering. Lecture Notes in Mechanical Engineering*. Springer, Singapore. [https://doi.org/10.1007/978-981-15-8025-3\\_30](https://doi.org/10.1007/978-981-15-8025-3_30).
- Alam, M. W.; Bhattacharyya, S.; Souayah, B.; Dey, K.; Hammami, F.; Rahimi-Gorji, M.; Biswas, R.** 2020. CPU heat sink cooling by triangular shape micro-pin-fin: Numerical study, *International Communications in Heat and Mass Transfer* 112: 104455. <https://doi.org/10.1016/j.icheatmasstransfer.2019.104455>.
- Hao, X.; Peng, B.; Xie, G.; Chen, Yi.** 2016. Efficient on-chip hotspot removal combined solution of thermoelectric cooler and mini-channel heat sink, *Appl Therm Eng.* 100:170-178. <https://doi.org/10.1016/j.applthermaleng.2016.01.131>.
- Wang, Y.; Zhu, K.; Cui, Z.; Wei, J.** 2019. Effects of the location of the inlet and outlet on heat transfer performance in pin fin CPU heat sink, *Applied Thermal Engineering* 151: 506–513. <https://doi.org/10.1016/j.applthermaleng.2019.02.030>.
- Beriache M.; Naji H.; Bettahar A.; Mokhtar Saïdia L.** 2012. Computation of thermal and hydraulic performances of minichannel heat sink with an impinging air jet for computer cooling, *Acta Polytechnica Hungarica* 9(2): 139-153. [http://acta.uni-obuda.hu/Beriache\\_Naji\\_Bettahar\\_Mokhtar-Saïdia\\_34.pdf](http://acta.uni-obuda.hu/Beriache_Naji_Bettahar_Mokhtar-Saïdia_34.pdf).
- Yang, Y.nT.; Lin, S. C.; Wang, Y. H.; Hsu, J. C.** 2013. Numerical simulation and optimization of impingement cooling for rotating and stationary pin–fin heat sinks, *Int. J. Heat Fluid Flow* 44: 383-393. <https://doi.org/10.1016/j.ijheatfluidflow.2013.07.008>.
- Huang, C. H.; Chen, Y. H.** 2014. An impingement heat sink module design problem in determining simultaneously the optimal non-uniform fin widths and heights, *Int. J. Heat Mass Transf.* 73: 627-633. <https://doi.org/10.1016/j.ijheatmasstransfer.2014.02.026>.
- Huang, C. H.; Chen, Y. H.** 2014. An optimal design problem in determining non-uniform fin heights and widths for an impingement heat sink module, *Appl. Therm. Eng.* 63: 481-494. <https://doi.org/10.1016/j.apptthermaleng.2013.11.008>.
- Yu, Y.; Simon, T. W.; Zhang, M.; Yeom, T.; North, M. T.; Cui, T.** 2014. Enhancing heat transfer in air-

- cooled heat sinks using piezoelectrically-driven agitators and synthetic jets, *Int. J. Heat Mass Transf.* 68: 184-193.  
<https://doi.org/10.1016/j.ijheatmasstransfer.2013.09.001>.
21. **Barrau, J.; Riera, S.; Leveille, E.; Frechette, L. G.; Rosell, J. I.** 2015. Nozzle to plate optimization of the jet impingement inlet of a tailored-width microchannel heat exchanger, *Exp. Thermal Fluid Sci.* 67: 81-87.  
<https://doi.org/10.1016/j.expthermflusci.2014.11.012>.
  22. **Byon, C.** 2015. Heat transfer characteristics of aluminum foam heat sinks subject to an impinging jet under fixed pumping power, *Int. J. Heat Mass Transf.* 84: 1056-1060.  
<https://doi.org/10.1016/j.ijheatmasstransfer.2015.01.025>.
  23. **Lin, S. M.; Liu, H. F.; Wang, W. R.; Lee, S. Y.; Cheng, C. Y.; Li, C. Y.** 2015. Optimum design and heat transfer correlation equation of a mini radiator with jet impingement cooling, *Appl. Therm. Eng.* 89: 727-737.  
<https://doi.org/10.1016/j.applthermaleng.2015.06.065>.
  24. **Xia, G.; Ma, D.; Zhai, Y.; Li, Y.; Liu, R.; Du, M.** 2015. Experimental and numerical study of fluid flow and heat transfer characteristics in microchannel heat sink with complex structure, *Energy Convers. Manage.* 105: 848-857.  
<https://doi.org/10.1016/j.enconman.2015.08.042>.
  25. **HoSung L.** 2011. *Thermal Design: Heat Sinks, Thermoelectrics, Heat Pipes, Compact Heat Exchangers, and Solar Cells.* John Wiley & Sons, Inc.
  26. **Maveety, J. G.; Hendricks, J. F.** 1999. A heat sink performance study considering material, geometry, Reynolds number with air impingement, *J. Electron. Packag.* 121: 156-161.  
<https://doi.org/10.1115/1.2792678>.
  27. **Maveety, J. G.; Jung, H. H.** 2002. Heat transfer from square pin-fin heat sinks using air impingement cooling, *IEEE Trans. Compon. Pack. Technol.* 25: 459-469.  
<https://doi.org/10.1109/TCAPT.2002.803650>.
- M. Beriache, B.H. Cherki, L. Mokhtar Saïdia, C. S. Nor Azwadi, M. Rizalman
- HEAT TRANSFER ENHANCEMENT THROUGH DIFFERENT HEAT SINK/IMPINGING AIR JET PARAMETERS AN EXPERIMENTAL APPROACH
- S u m m a r y
- In the present work, improving the thermal performance of a central processing unit (CPU) cooling system consisting of a plate fin minichannel heat sink exposed to an air jet of impact is accomplished. The height of the impinging air jet duct, the mode of air flow on the heat sink, air blowing mode and as well as the suction blow mode "pull" and the air jet duct geometry are three important influence parameters on the phenomenon. The results obtained show that a jet height  $H = 20$  mm, a convergent duct of  $H = 40$  mm in height and a hair dryer tip provide further improvement of the cooling technique. The two preceding parameters combined with the fan air suction blow mode improve the performance by at least 11,2% compared to the initial configuration (marketed product), having as characteristics ( $H = 0$  mm, fan in the blowing push mode). The use of a converging duct and a hair dryer conduit show that the velocities from the hair dryer tip far exceed those from the best standard conduit height,  $H = 20$  mm. That said, the improvement of the flow in the central zone is substantially achieved, which consequently improves the heat removal in this zone at least 19%.
- Keywords:** electronic cooling, CPU, impinging air jet, heat sink, thermal resistance.

Received June 26, 2022

Accepted January 27, 2023



This article is an Open Access article distributed under the terms and conditions of the Creative Commons Attribution 4.0 (CC BY 4.0) License (<http://creativecommons.org/licenses/by/4.0/>).